Thermo-structural fatigue and lifetime analysis of a heat exchanger as a feedwater heater in power plant

Siamak Hoseinzadeh* and P. Stephan Heyns

Centre for Asset Integrity Management, Department of Mechanical and Aeronautical Engineering, University of Pretoria, Pretoria, South Africa

*Corresponding author.

Hosseinzadeh.siamak@up.ac.za

Hoseinzadeh.siamak@gmail.com

Highlights

- The real design of a shell-and-tube counter-flow heat exchanger as a feedwater heater in power plant is considered.
- Failure conditions are evaluated according to the ASME VIII Boiler and Pressure Vessel Code.
- The results of equivalent thermal stress analysis and system lifetime under two extreme loading conditions are reported.
- The highest equivalent thermal stresses occur at the joints of the tubes and tubes sheet and is equal to 641 and 931 MPa, respectively.
- The lifetimes of tubes and tube sheets are 10^5 and 10^4 cycles respectively for the valley and peak load conditions.

Abstract

Today, the use of shell and tube heat exchangers has become widespread and they are used in various industries under very diverse operating conditions. Specific operating conditions make it possible to consider and simulate the operating terms and failure conditions of these converters. In this study, the design of a shell-and-tube counter-flow heat exchanger in AutoCAD software is first considered, and the system is then meshed and simulated in ANSYS 2019 software. Simulation results of temperature, pressure, heat flux and fluid velocity within the system are reported in order to understand the system performance. Failure conditions are evaluated according to the ASME VIII Boiler and Pressure Vessel Code, and the results of equivalent thermal stress analysis and system lifetime under two extreme loading conditions are reported. The highest equivalent thermal stresses under these extreme load conditions occur at the joints of the tubes and tubes sheet and is equal to 641 and 931 MPa, respectively. Also, the lifetimes of tubes and tube sheets are 10^5 and 10^4 cycles respectively for the valley and peak load conditions.

Keywords: Heat exchanger; Equivalent thermal stress; Fluid simulation; Fatigue; Lifetime analysis

1. Introduction

Today, the use of shell and tube heat exchangers has dramatically grown in many industries, and they are found in the production of electricity, oil, etc. Other applications include heating and air conditioning, chemical processes, desalination, and food preservation [1], [2], [3], [4], [5]. Since industrial converters face very high temperatures and pressures when operating, it is essential to analyze the effects of high temperatures and pressures, as well as the stress and fatigue of these mechanical components [6], [7], [8], [9], [10]. Therefore, predicting fatigue and creep life is critical for heat exchangers [11], [12].

Pande et al. [13] analyzed and determined the fatigue life of tube sheets which are widely used in filters, as the main elements of filter tube support. They also predicted fatigue life with the ASME codes. Raj et al. [14] investigated the effects of different fluid flow gradient angles and heat transfer characteristics of shell and tube heat exchangers, for three different baffle inclination angles, namely 0°, 10° and 20°. Arora et al. [15] investigated fatigue crack growth behavior in austenitic stainless steel tubes and welded tubes and obtained predicted and experimental results. Then they used the Paris law to predict the fatigue life. Booysen et al. investigated a sequential method used to predict the fatigue life of a low-pressure steam turbine blade during resonance conditions during turbine startup. [16]. Farrahi et al. [17], [18] explored ways of maintaining the thermal and mechanical integrity of shell and tube heat exchangers, by passing a series of rods through tubes which were welded to tubesheets from both ends. Gupta et al. [19], presented an experimental investigation of heat transfer and pressure drop characteristics, for R-134a condensing inside a horizontal helical tube while cooling water flows through the shell. Solanki et al. [20] investigated condensation heat transfer coefficients and friction pressure of R-134a inside a micro-fin helical coil tube with cooling water flowing inside the shell in the opposite direction [20]. Ozden et al. [21] investigated the design of the shell side of a shell and tube heat exchanger. They considered parameters such as baffle distance, baffle cut, and the dependence of shell diameter on heat transfer coefficient and pressure drop through numerical simulation. Rondon et al. [22] studied fatigue evaluation of shop welded flat bottom tanks based on the API specification using finite element analysis with shell models, axisymmetric models and solid sub-models to determine stress components and stress tensor ranges, and to obtain effective alternating equivalent stress. In their work, Shiraiwa et al. [23] investigated ways of improving the performance of the highly efficient heat exchange obtained in falling film type heat exchangers, and reported results for in-tube conditions. Wajs et al. [24] presented results obtained for a patented heat exchanger design with minijets and a cylindrical construction. The results are based on systematic experimental investigations in the single-phase convection heat transfer mode. In this method, the shell and tube heat exchangers are divided into several series of heat exchangers and the Tubular Exchanger Manufacturers Association (TEMA) standards are strictly followed. Patil et al. [25] describe a way by which thermal fatigue can be accurately identified and analyze fatigue in pressure vessels in accordance with a design by analysis method. The research highlights different failure modes and the design by analysis approach used for a pressure vessel. This capability allows the engineer to examine a wide range of variables during the design process and ensure a safe design [26].

In this research, the operating conditions for a high-pressure shell and tube heat exchanger are examined and simulated, using a feedwater heater in a powerplant as example. First, the system is investigated in terms of operating conditions such as pressure and temperature as well as failure conditions like the equivalent thermal stress and fatigue. The design of the system in AutoCAD and simulation in ANSYS 2019 is presented, with the relevant equations

from the ASME VIII Code. The results are then reported in terms of temperature, pressure, fluid flux, and velocity analysis. The thermal stress equivalent and the fatigue lifetime of the system are also reported. The study method for analysis of equivalent thermal stress is the von Mises method and for lifetime is the signed von Mises method, which is performed by ANSYS software.

2. System description

The system is a counter-flow shell and tube, high-pressure heat exchanger such as a feedwater heater. The AutoCAD software was used to draw the plan of this heat exchanger. The heat exchanger is an integrated system, but it can be broken down into ends and tubes for simplicity. Initially, the end part of the system consisted of the feeding water inlet to tubes and the outlet of feeding water from the tubes. This part has two hollow cylinders with radii of 1320 mm and 1044 mm, respectively. The length of this part is 1074 mm. The inlet and outlet nozzles of feed water are 300 mm in diameter. Their length is 502 mm. The end of the segment, including end shell, the feed inlet and outlet of the feed, and two supports are shown in Fig. 1.

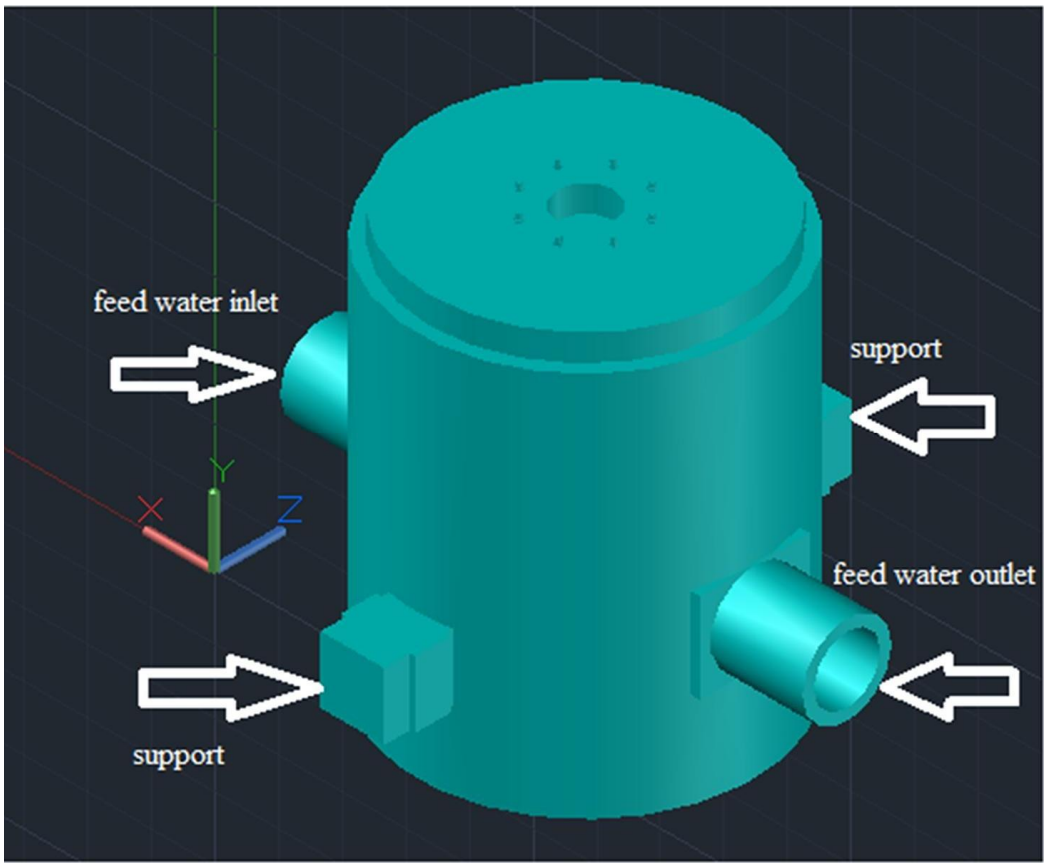

Fig 1. End of segment, including end shell, feed inlet and outlet of feed and two supports.

A tube sheet also separated the inlet and outlet from an inlet of the feedwater heater. This tube sheet is shown in Fig. 2.

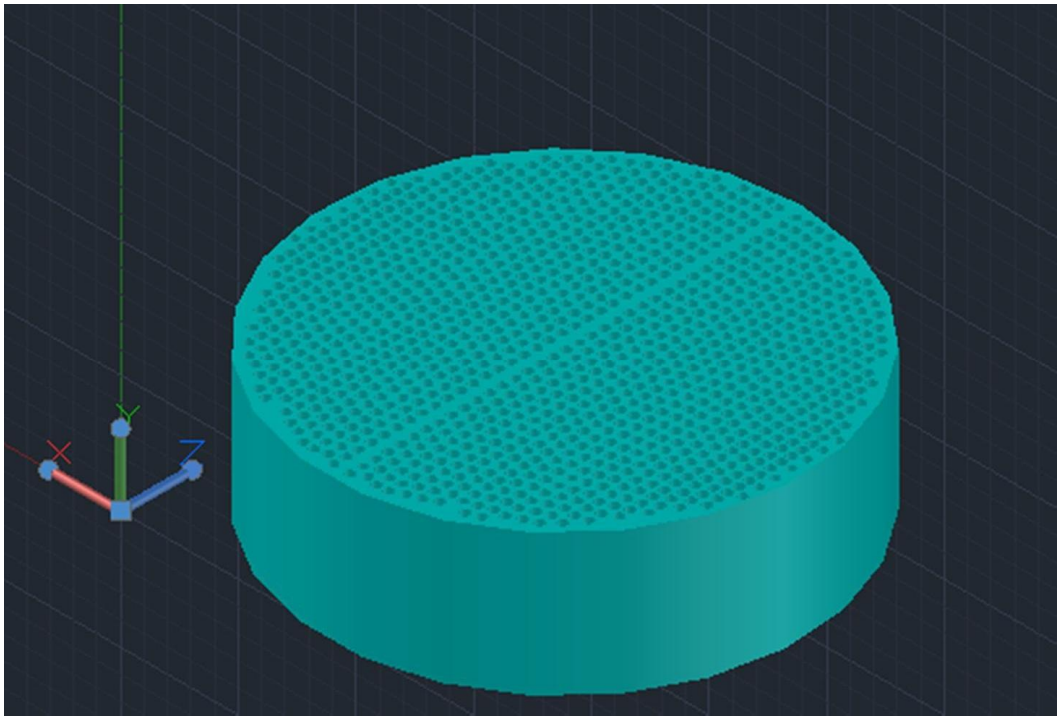

Fig 2. Tube sheet of feedwater heater.

The other part of the system consists of two hollow cylinders, and there are two nozzles representing the inlet and outlet of the feedwater heater. Also, there are 1120 U-shaped tubes in the cylinders. Fig. 3 shows tubes in the shell with nozzles for the inlet and outlet of the feedwater heater.

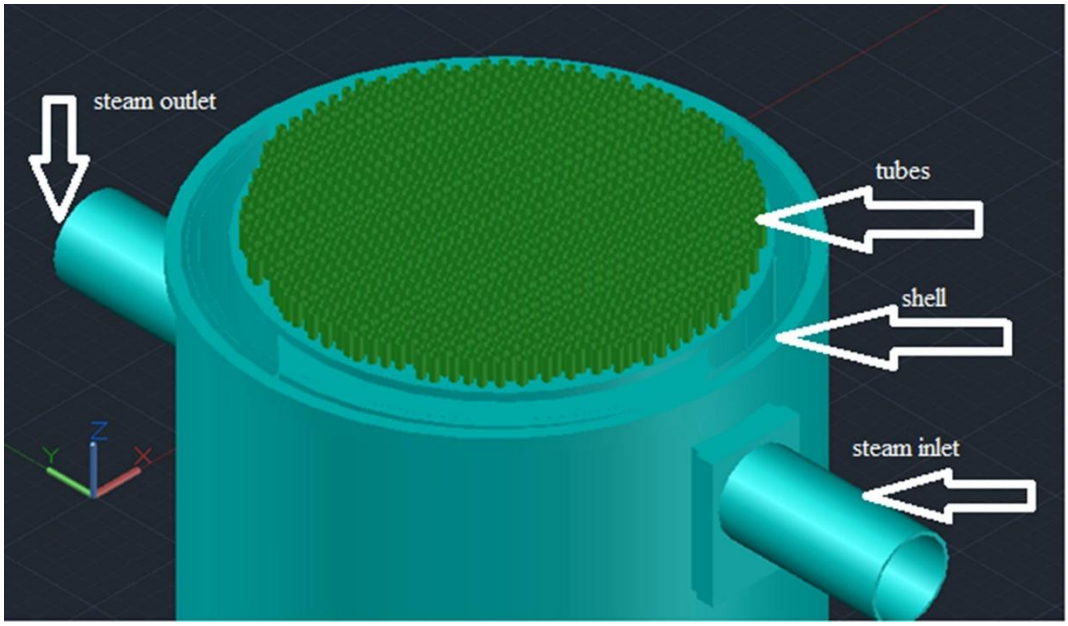

Fig 3. Tubes drawn in shell with nozzles for inlet and outlet of water heater.

These components are then interconnected and integrated. Fig. 4 shows the whole system seamlessly.

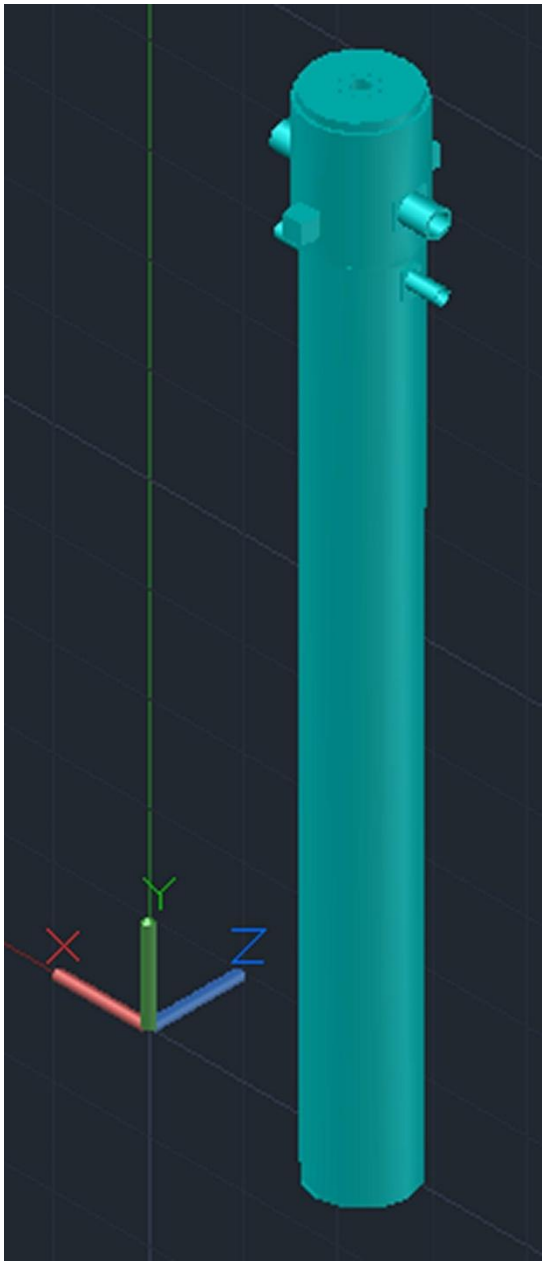

Fig 4. The whole system seamlessly.

3. System simulation

The system was simulated by ANSYS 2019 software. First, the system was meshed. Since the system is actually very large, the assumptions underlying the system simulation are as follows:

1. The overall length of the system was reduced to an initial length of 0.25 m (both shell and tubes).
2. Since the system is symmetric, the symmetry condition is used to simulate.
3. Since the whole process inside the tubes is almost the same in each tube, the number of tubes has been reduced to 55.

The geometry after simulation is shown in Fig. 5.

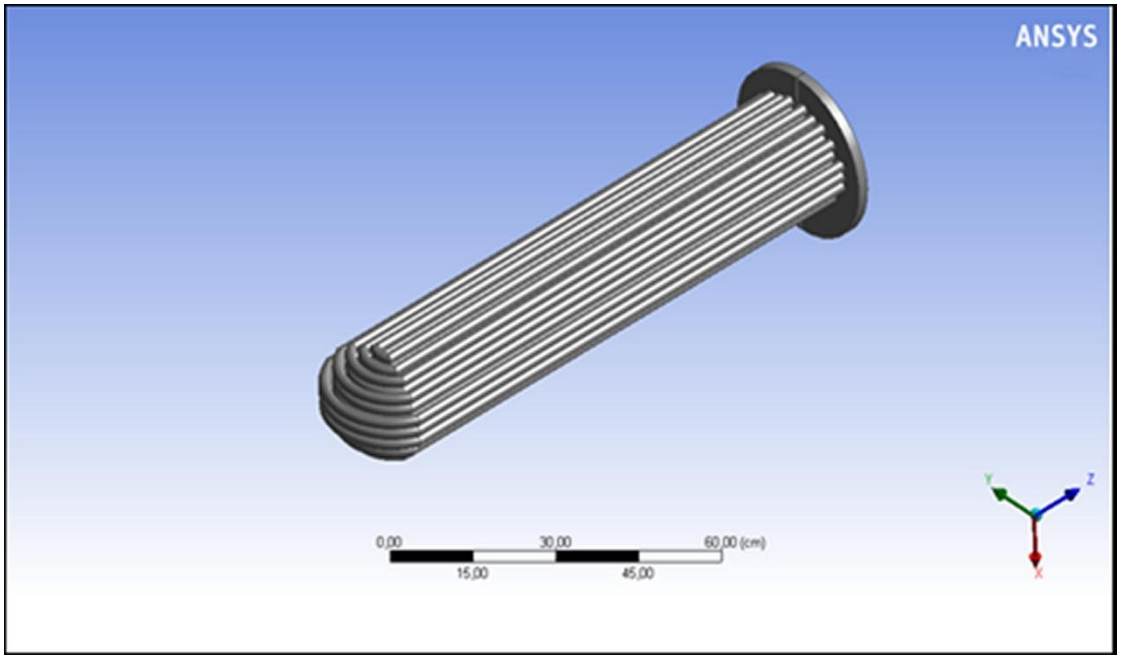

Fig 5. Final geometry after simulation.

The type of mesh element is tetrahedrons. The number of mesh elements is 2824920. The quality of elements is not compromised by the failure of elements or sharp angles, etc.

The quality of the mesh was determined by a criterion called skewness, the quality is shown in Fig. 6, and classification of the type of condition is reported in Table 1.

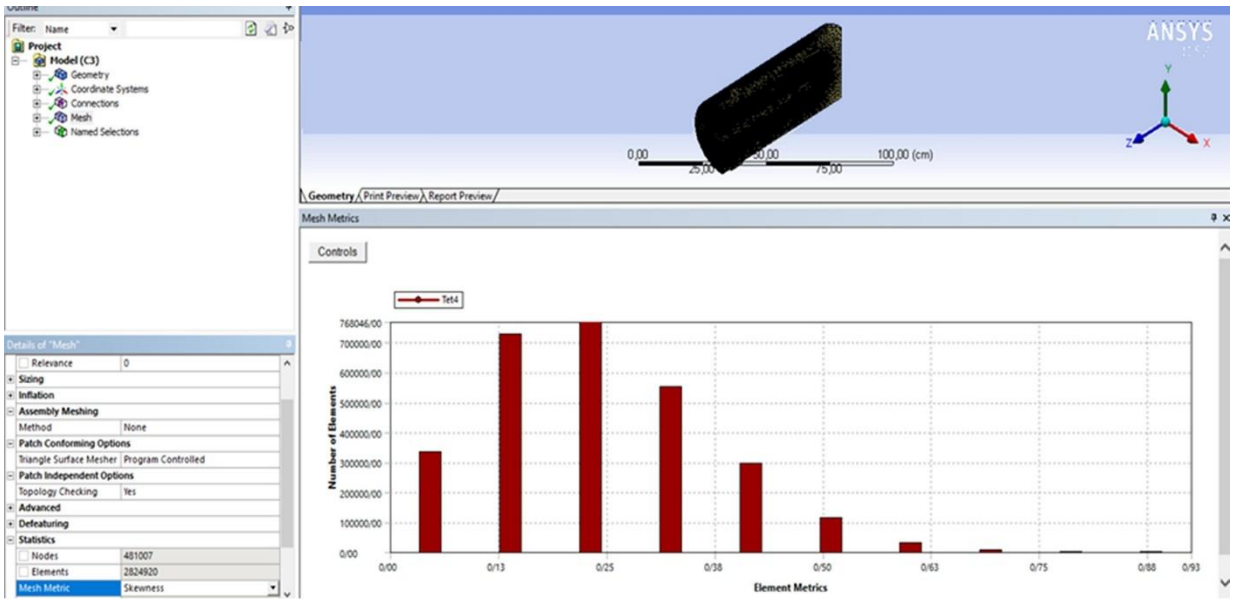

Fig 6. The value of skewness.

Table 1. Classification of type of quality of skewness.

Skewness	Cell quality
1	degenerate
0.9 - <1	bad
0.75–0.9	poor
0.5–0.75	fair
0.25–0.5	good
>0–0.25	excellent
0	equilateral

By comparing Fig. 6 and Table 1, it is evident that the number of meshed elements which are in the proper range 0.0 to 0.5 are very high and this indicates a large number of high quality meshes.

The system as meshed is shown in Fig 7, Fig 8.

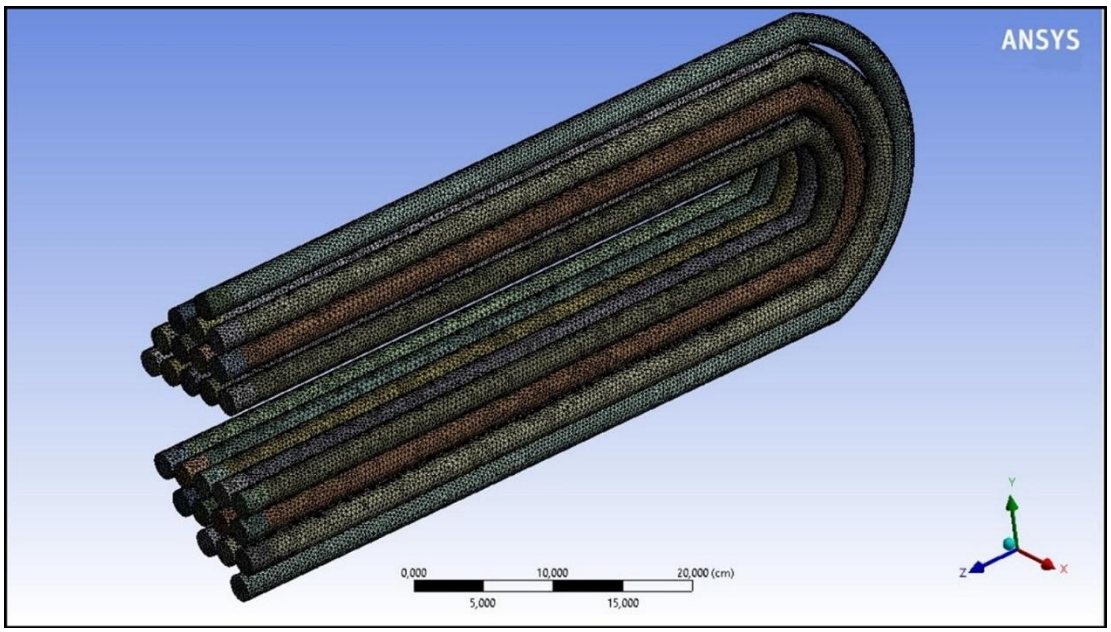

Fig 7. Overview of tube meshes.

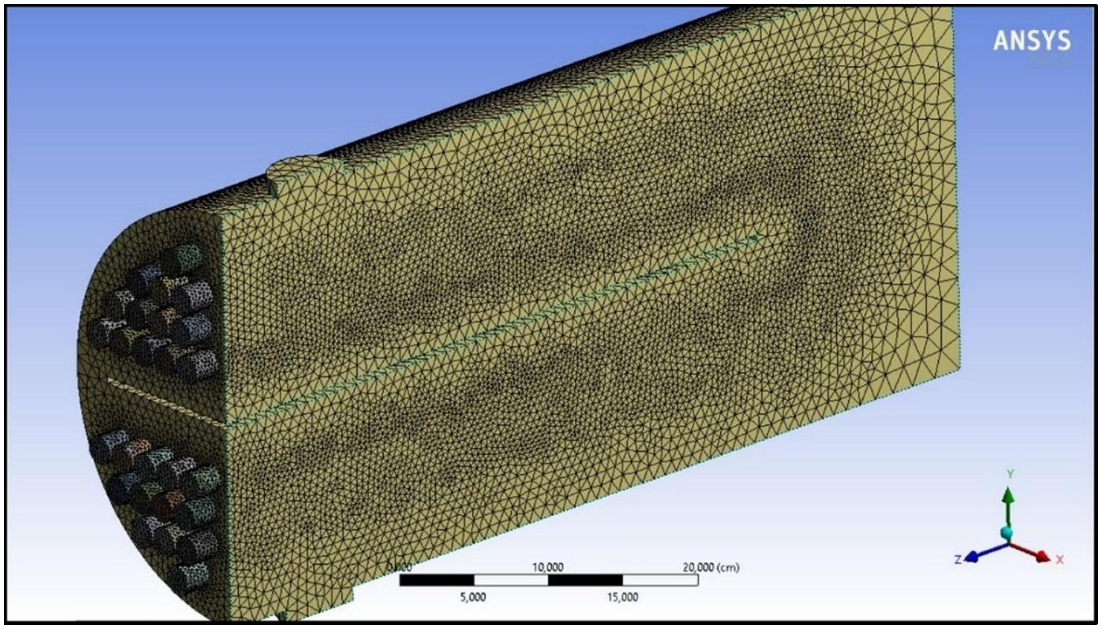

Fig 8. Overview of system including tubes and tube sheet and shell meshes.

In order to investigate the mechanical conditions of the system, the pressure, temperature, heat flux, and velocity contours were investigated and described. The design parameters and initial conditions for the system are given in Table 2.

Table 2. Design parameters and initial conditions for the system.

Section	Inlet temperature (K)	Inlet pressure (bar)	Mass flow rate (kg/s)
Shell (steam)	693	19.91	12.455
Tube (feed water)	443.5	193	177.95

Fig. 9 shows how the heat flux changes through the system.

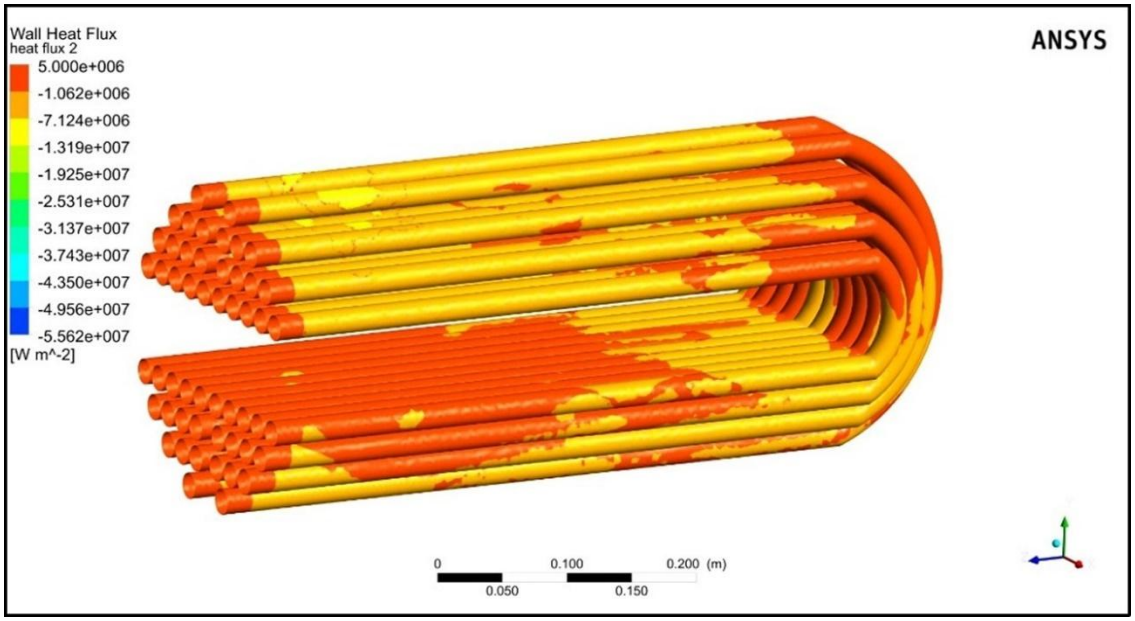

Fig 9. The system heat flux contour.

As shown in Fig. 9, the heat flux in tubes gradually decreases, although in the U-section, a sudden increase is observed.

Fig. 10 shows how the temperature through the system changes.

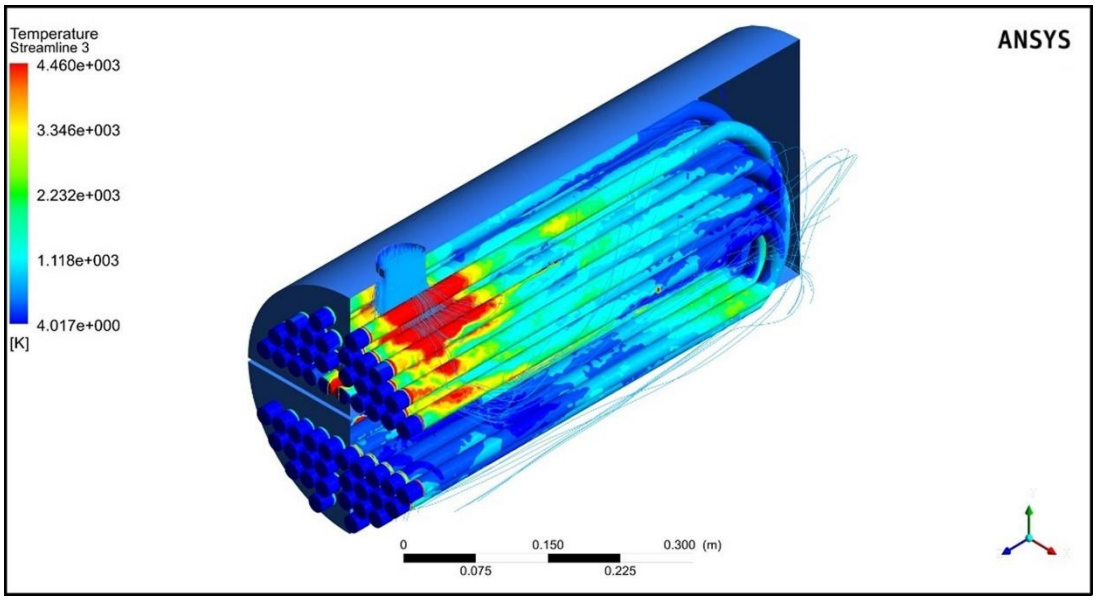

Fig 10. The system temperature contour.

As shown in Fig. 10, the temperature at end of tubing is higher than at the beginning.

4. Fatigue evaluation – Elastic stress analysis

Fatigue analysis was performed to evaluate the number of operating cycles that the equipment can withstand prior to failure.

4.1. Fatigue cycles

Intermittent stresses occur in the heat exchanger due to startup and shutdown of the heat exchanger cycle. These stresses are investigated here to determine the permissible number of cycles. The following two conditions illustrate peak and valley conditions for fatigue assessment.

- The water inside the tubes has a temperature of 443.5 K and the water inside the tubes has a temperature of 693 K. At startup, the pressure inside the tubes is equal to ambient pressure, and the pressure inside the shell is 19.91 bar. This is called the valley point.
- After reaching a steady state after a few hours, the temperature inside the tubes reaches 500 K, and the water inside the shell reaches 650 K. Under stable system conditions, the water pressure inside the tubes is 193 bar, and the pressure inside the shell is considered to be 19.91 bar. This is called the peak point
- These conditions simulate the maximum temperature gradient and hence the maximum intermittent heat stress. Therefore, alternating equivalent stress in each node is calculated from the integration of thermal and compressive stress and is equal to the maximum transient stress.

4.2. Thermal and structural loads

Structural loads on systems include pressure loads, deadweight, and nozzle loads. Only pressure loads are considered in the present analysis. The lateral pressure of shell and tubes together with compensating pressure are applied to the inner surface of the shell and tubes, respectively.

Thermal loads include shell and tube side temperatures. These loads (A and B) referring to (peak and valley) load cases are summarized in Table 3.

Table 3. Thermal and structural loads.

Load cases		Tube side	Shell side
Thermal	Valley (A)	443.5 K	693 K
	Peak (B)	500 K	650 K
Structural	Valley (A)	ambient pressure	19.91 bar
	Peak (B)	193 bar	19.91 bar

4.3. Effective alternating equivalent stress range

The effective equivalent stress range was calculated by using the alternating stress equation. The component stress amplitude and the effective equivalent stress amplitude for the start and end points were calculated by using the following method:

The von Mises stress criteria equations were used to determine the equivalent structural and thermal stress equivalents.

$$\Delta\sigma = (\sigma_{11} - \sigma_{11}^{LT})_m - (\sigma_{11} - \sigma_{11}^{LT})_n \quad (1)$$

$$(\Delta S_{p,k} - \Delta S_{LT,k}) = \frac{1}{\sqrt{2}}\left[(\Delta\sigma_{11} - \Delta\sigma_{22})^2 + (\Delta\sigma_{11} - \Delta\sigma_{33})^2 + (\Delta\sigma_{22} - \Delta\sigma_{33})^2 + 6\,(\Delta\sigma_{12}^2 + \Delta\sigma_{13}^2 + \Delta\sigma_{23}^2)\,0.5\right] \quad (2)$$

Similar to the above, the local heat equivalent stresses at the start and end time were calculated using the following equations:

$$\Delta\sigma_1^{LT} = \sigma_1^{mLT} - \sigma_1^{nLT} \quad (3)$$

$$\Delta S_{LT,k} = \frac{1}{\sqrt{2}}\left[(\Delta\sigma_1^{LT} - \Delta\sigma_2^{LT})^2 + (\Delta\sigma_1^{LT} - \Delta\sigma_3^{LT})^2 + (\Delta\sigma_2^{LT} - \Delta\sigma_3^{LT})^2\right]^{0.5} \quad (4)$$

Then, after evaluating the stress component amplitude of system component, the effective alternating equivalent stress amplitude for system was also calculated.

Equation (5) was used to determine the alternating stress in the system:

$$S_{alt,k} = \frac{k_f * k_{e,k} * (\Delta S_{p,k} - \Delta S_{LT,k}) + k_{v,k} * \Delta S_{LT,K}}{2} \quad (5)$$

In the above equation k_f is the fatigue strength reduction factor, $k_{e,k}$ is the fatigue penalty factor, $k_{v,k}$ is the Poisson correction factor , $\Delta S_{LT,k}$ is the local thermal equivalent stress and $\Delta S_{p,k}$ is the reduction in fatigue strength called k_f. This factor depends on the type of welding and the surface area of the heat exchanger as well as the examination performed on the welds.

A 1.7 fatigue strength reduction factor was assigned for computation for fillet welds. In order to obtain the fatigue penalty $k_{e,k}$, which is calculated as the main factor of secondary equivalent stress amplitude, stress linearization in stress peak areas was used to classify stresses [26].

The amplitude of the primary equivalent plus the secondary equivalent stress is lower than permissible limit, so $k_{e,k}$ is considered to be 1.

$k_{e,k} = 1$ for $\Delta S_{n,k} \leq S_{PS}$

Also Poisson's correction factor is assumed to be 0.3.

4.4. Permissible number of cycles and fatigue damage

The alternating stresses obtained by Equation (1) were used to calculate the number of cycles allowed [26].

The fatigue design curves of smooth strips is a polynomial function that depends on the properties of the material and the range of stress at a specific temperature.

Eqs. (6), (7), (8) are used to determine the permissible number of heat exchanger equipment cycles.

$$N = 10^X \quad (6)$$

$$X = \frac{C_1 + C_3\ Y + C_5\ Y^2 + C_7\ Y^3 + C_9\ Y^4 + C_{11}\ Y^5}{1 + C_2\ Y + C_4\ Y^2 + C_6\ Y^3 + C_8\ Y^4 + C_{10}\ Y^5} \quad (7)$$

$$Y = \left(\frac{E_T}{E_{FC}}\right) * \left(\frac{S_a}{C_{us}}\right) \quad (8)$$

In the equations above, $C_1 \ldots C_{10}$ are material constants of the system, selected separately and put into the equation, S_a is the alternating equivalent stress , E_T is the modulus of elasticity of the material under evaluation at the average temperature of the cycle being evaluated, E_{FC} is the modulus of elasticity used to establish the design fatigue curve, N is the number of allowable design cycles, X is the exponent used to compute the permissible number cycles and C_{us} is the conversion factor.

Therefore, the number of cycles allowed before failure of the system can be obtained. In addition, fatigue is calculated according to Eq. (9) as the ratio of the actual number of cycles to the number of cycles allowed.

$$D_f = \left(\frac{n}{N}\right) \quad (9)$$

where n is the number of cycles for the heat exchanger.

The ANSYS Workbench software was used to evaluate the stress range and alternating stress range and lifetime of the system [27], [28], [29].

5. Results and discussion

After analyzing temperature, pressure, heat flux, and thermal stress in the system, the results of thermal stress and lifetime on the tube sheet and shells were reported. The equivalent stresses on the tube sheet and the shell due to the loads reported in Table 3 are shown for the two loading cases A and B in Fig 11, Fig 12, Fig 13, Fig 14. The von Mises method was used to obtain equivalent stress. Fig. 11 shows the equivalent thermal stress on the tube sheet for load A. The equivalent thermal stress is distributed uniformly on the tube sheet. However, in some places, such as the connections between the tube and tube sheet, the thermal stress is higher. Fig. 12 shows the equivalent thermal stress on the shell of the system due to load A. The equivalent thermal stress is distributed uniformly on the shell. However, in some places, such as the connections between the shell and support, the thermal stress is higher. Because the system is supported in these areas and because of the weight, the thermal stress system is higher. The maximum equivalent thermal stress in these conditions is approximately 641 MPa.

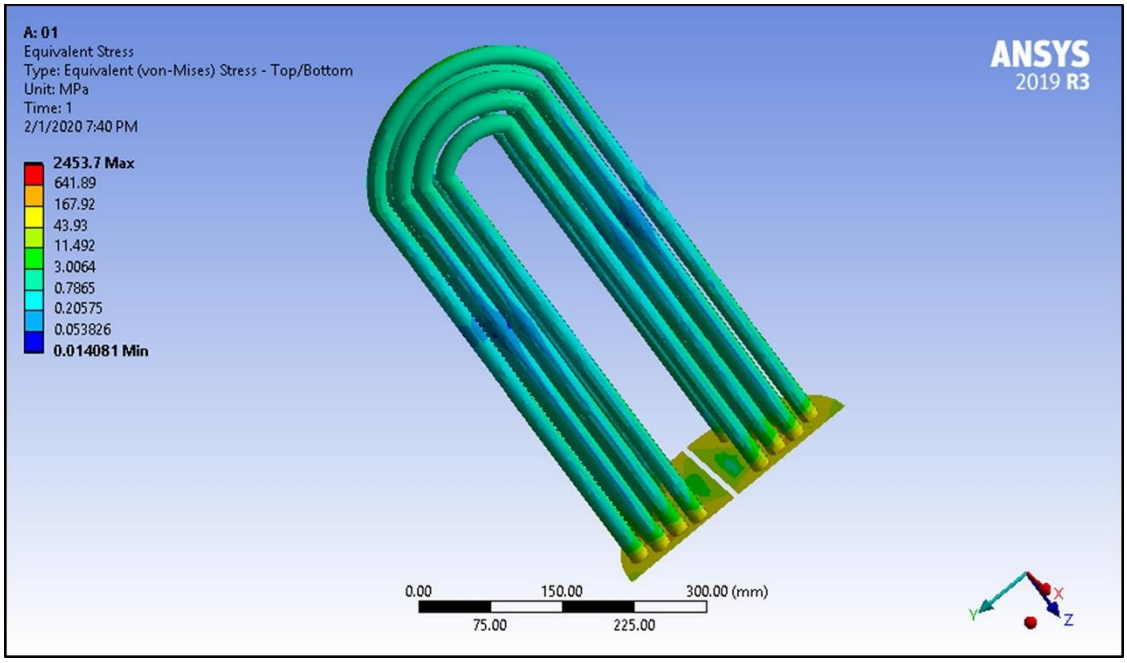

Fig 11. Equivalent thermal stress on tubesheet in loading A.

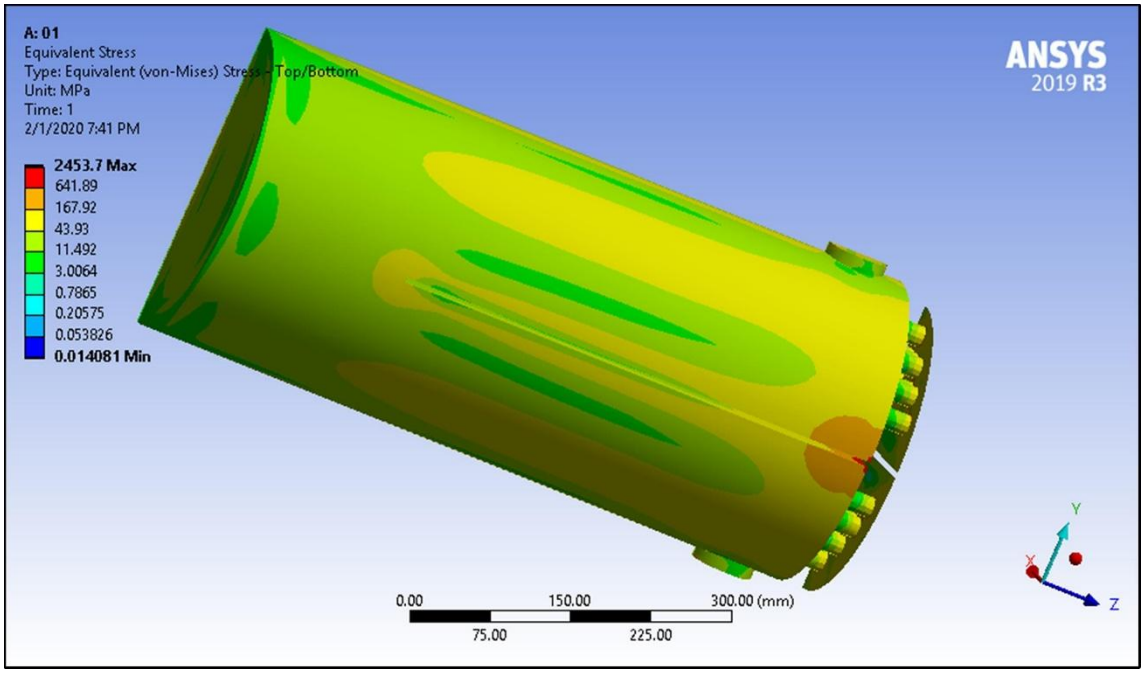

Fig 12. Equivalent thermal stress on shell of system in loading A.

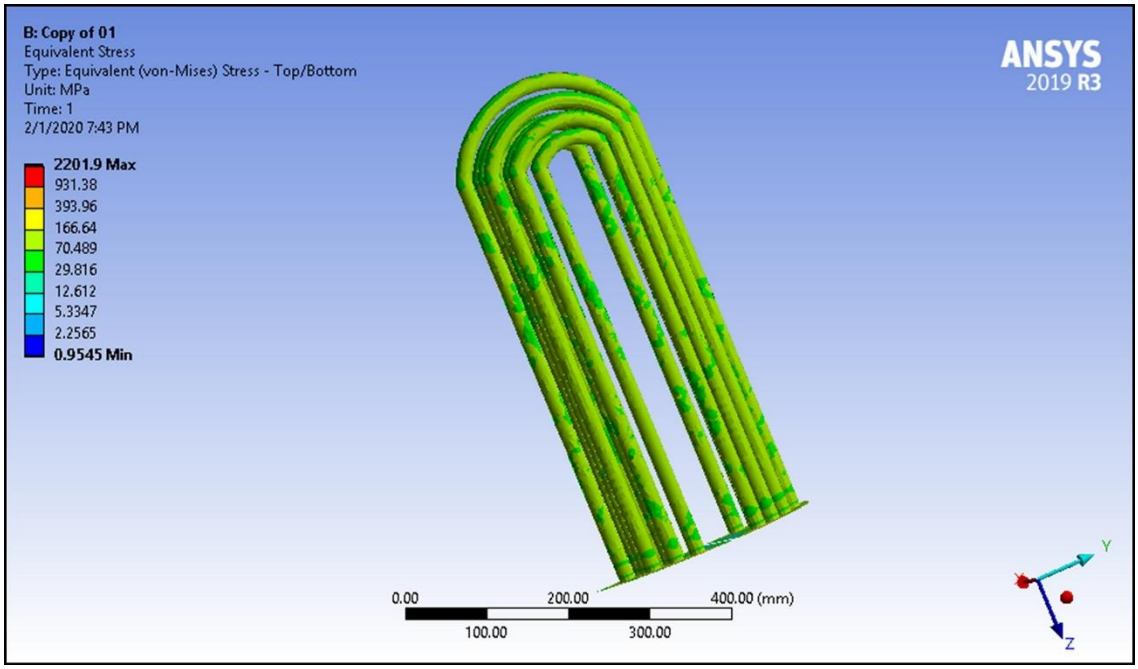

Fig 13. Equivalent thermal stress on tubesheet in loading B.

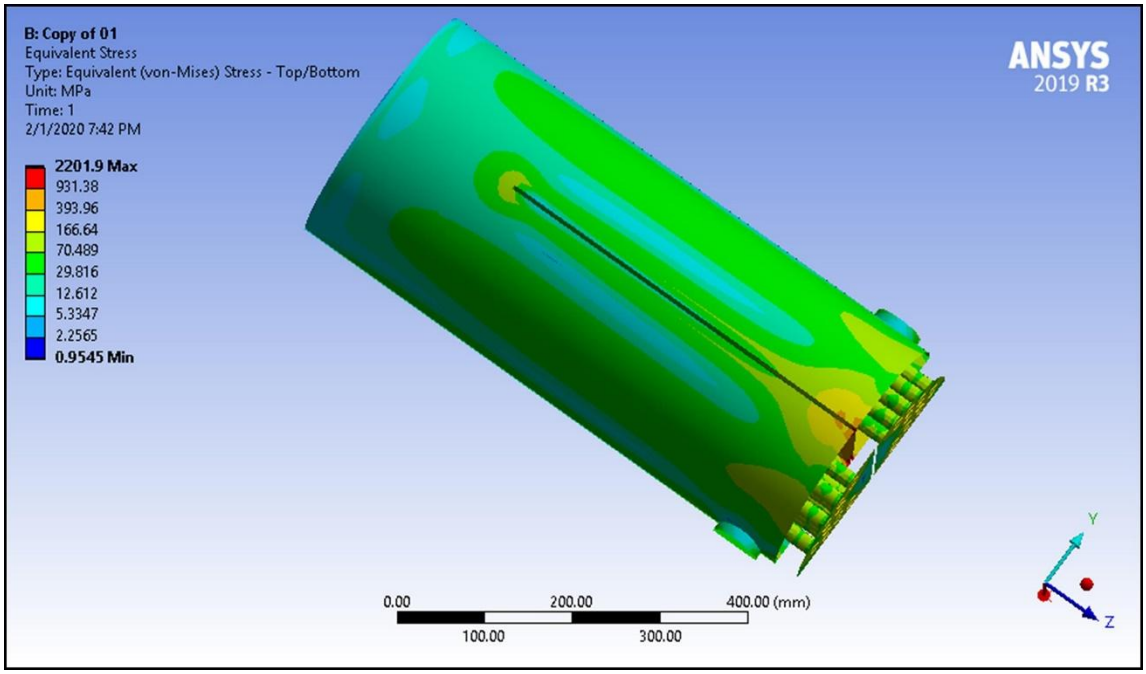

Fig 14. Equivalent thermal stress on shell of system in loading B.

Fig. 13 shows equivalent thermal stress on tube sheet in load B. The equivalent thermal stress is distributed uniformly on the tube sheet. However, in some areas, such as the connections between the tube and tube sheet, the thermal stress is higher. Fig. 14 shows equivalent thermal stress on the shell of system in load B. The equivalent thermal stress is distributed uniformly on the shell. However, in some areas, such as the connections between the shell and support, the thermal stress is higher. The maximum equivalent thermal stress under these conditions is approximately 931 MPa. By comparing the equivalent thermal stress at for load cases A and B, it was found that for B, the equivalent thermal stress is greater in both the tube plate and the shell.

The lives (number of cycles allowed before failure) for the two load cases A and B are reported in table 3 on the tube sheet, and the shell in Fig 15, Fig 16, Fig 17, Fig 18. The signed von Mises stress can be calculated by using user-defined results. This stress sign could be directly multiplied by the unsigned von Mises stress to produce the signed von Mises stress. The signed von Mises method was used to obtain the fatigue lives of the system sections. The unit of the values presented in Fig 15, Fig 16, Fig 17, Fig 18 is the number of cycles that the system can withstand without failure.

Fig. 15 shows the fatigue life of the tube sheet for load case A. The longer service life of the system is reported to be 10^8 cycles of loading. As shown in Fig. 16, it is observed that the life of connecting parts between tubes and the tube sheet is shorter than the other components, and it's about equal to 10^5 cycles of loading, and these points are more sensitive.

Fig. 15 shows the life of the system's shell under load A. The lifetime of most parts of the shell is 10^6 cycles of loading. It has also been observed that the support portion has the lowest life expectancy. Because of these parts, there is system support. And because of the weight-bearing system and connections, the lifetime at these points is shorter.

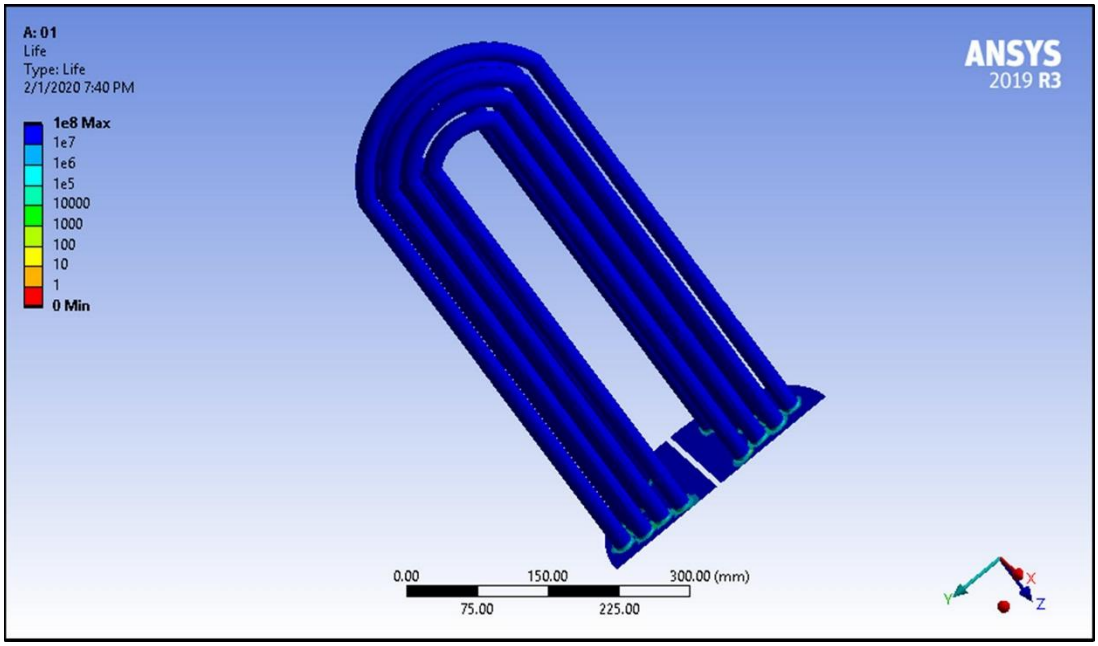

Fig 15. Life of tube sheet in loading A.

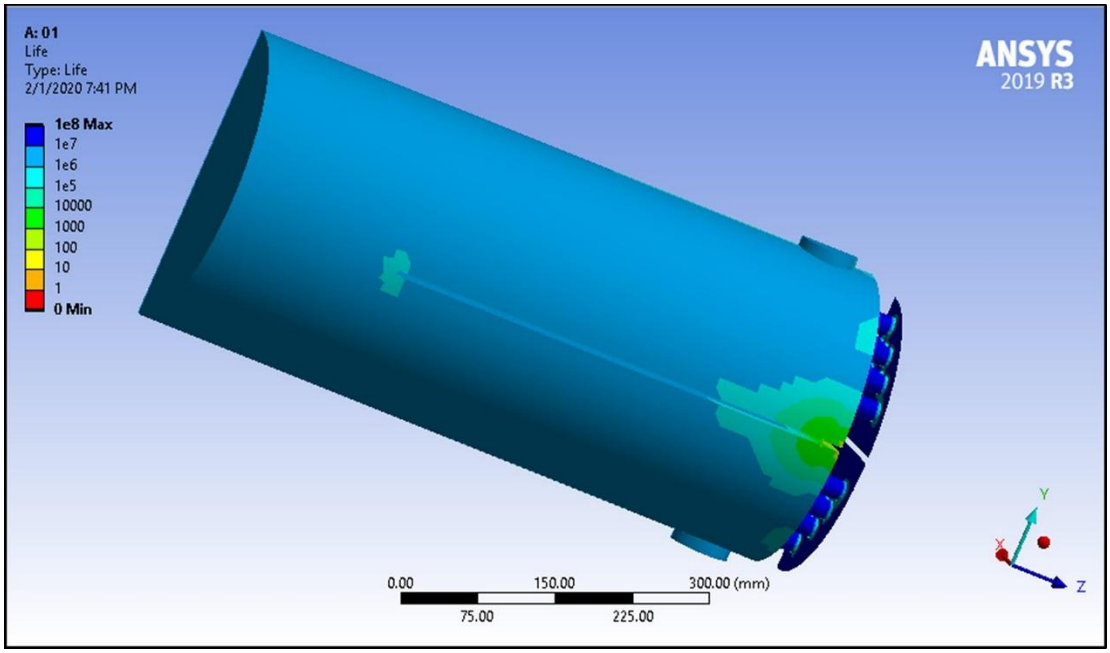

Fig 16. Life of system's shell in loading A.

The longer service life of the system was reported to be 10^7 cycles of loading. As shown in Fig. 17, it is observed that the life of the connecting parts between the tubes and the tube sheet is shorter than the other components, and it is about 10^5 cycles of loading, and these points are more sensitive.

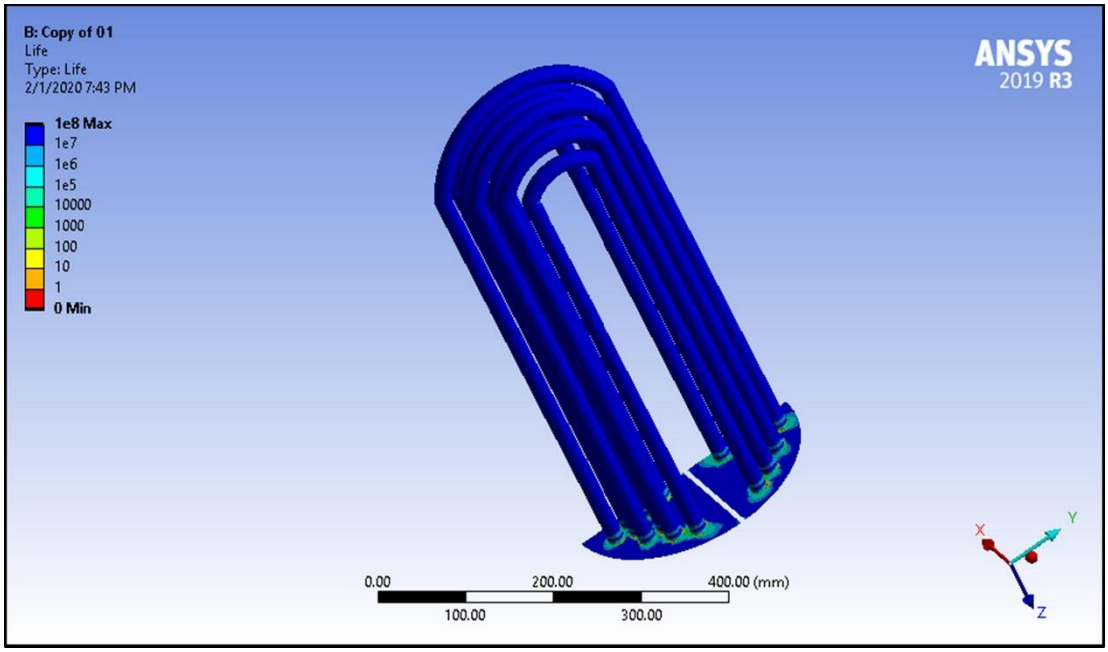

Fig 17. Life of tube sheet in loading B.

Fig. 18 shows the life of the shell in load case B. The longevity of most parts of the shell is 10^6 cycles of loading. It can also be seen that the support area has the lowest life expectancy.

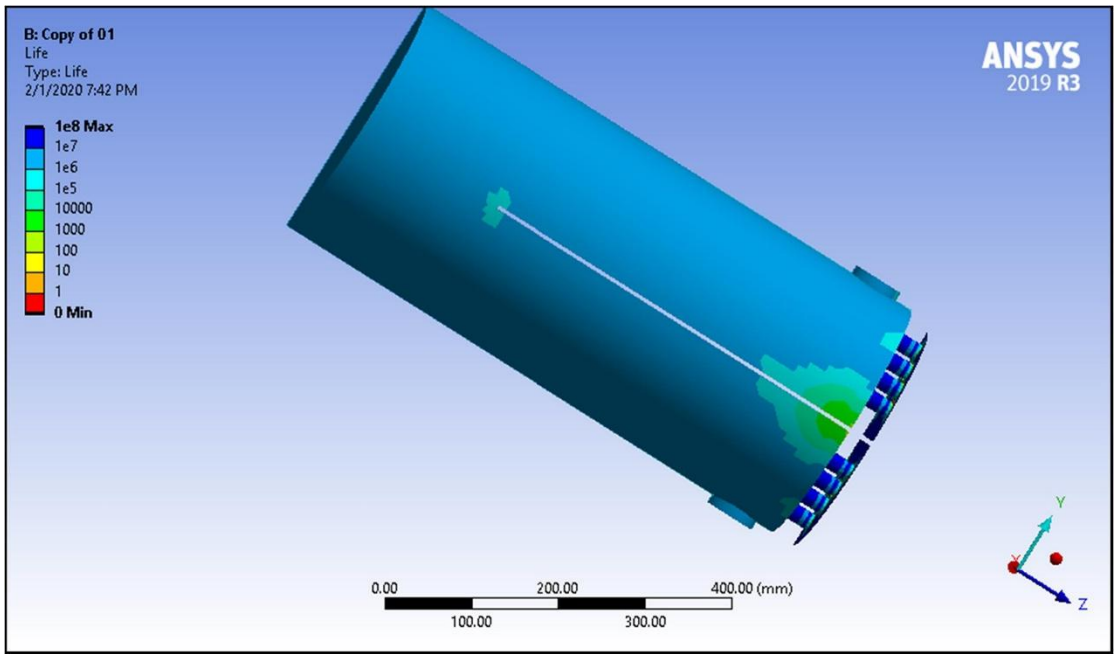

Fig 18. Life of system's shell in loading B.

After analyzing the results of the equivalent thermal stress of the system and the lifetime of the system components, it may be concluded that the most sensitive parts of the system are the connecting points between the tubes and the tube sheet and the supports which have the shortest lifetime and the highest heat stress equivalent. As expected may also be observed that the system has a shorter lifetime during peak loading.

6. Conclusion

In this study, the high-pressure shell and tube heat exchanger system of a typical counter-flow feedwater heater for a power plant is considered. The system was meshed in ANSYS, and the pressure, temperature, heat flux, and velocity contours were analysed and reported. In addition the governing equations of the system are presented. In order to investigate the system lifetime, equivalent thermal stress analyses were conducted with the ASME VIII Boiler and Pressure Vessel Code were performed for two extreme load cases. The results show that the critical points of the system are those parts of the tubes connected to the tube sheet, because they have the highest thermal stress and the shortest lifetime. The thermal stresses of the joints of the tube sheet and tube joints for the two load cases conditions are 641 and 931 MPa, respectively. The lifetimes of these components for the peak and valley peak loading conditions are 10^5 and 10^4 cycles, respectively.

Declaration of Competing Interest

The authors declare that they have no known competing financial interests or personal relationships that could have appeared to influence the work reported in this paper.

Acknowledgements

The authors would like to acknowledge the support provided by Mr. Gary de Klerk.

References

[1] S. Hoseinzadeh, R. Azadi. Simulation and optimization of a solar-assisted heating and cooling system for a house in Northern of Iran. J. Renew. Sustain. Energy, 9 (2017), 10.1063/1.5000288
[2] S. Hoseinzadeh, M. Hadi Zakeri, A. Shirkhani, A.J. Chamkha. Analysis of energy consumption improvements of a zero-energy building in a humid mountainous area. J. Renew. Sustainable . (2019), p. 11, 10.1063/1.5046512
[3] M.E. Yousef Nezhad, S. Hoseinzadeh. Mathematical modelling and simulation of a solar water heater for an aviculture unit using MATLAB/SIMULINK. Journal of Renewable and Sustainable. Energy., 9 (2017), 10.1063/1.5010828
[4] S. Hoseinzadeh, R. Yargholi, H. Kariman, P.S. Heyns. Exergoeconomic analysis and optimization of reverse osmosis desalination integrated with geothermal energy. Environ. Prog. Sustain. Energy (2020), 10.1002/ep.13405
[5] H. Kariman, S. Hoseinzadeh, A. Shirkhani, P.S. Heyns, J. Wannenburg. Energy and economic analysis of evaporative vacuum easy desalination system with brine tank. J. Therm. Anal. Calorim. (2019), 10.1007/s10973-019-08945-8
[6] Yari, A., Hosseinzadeh, S., Golneshan, A. A. & Ghasemiasl, R. Numerical simulation for thermal design of a gas water heater with turbulent combined convection. in ASME/JSME/KSME 2015 Joint Fluids Engineering Conference, AJKFluids 2015 1A, (American Society of Mechanical Engineers, 2015).
[7] S. Hoseinzadeh, S.A.R. Sahebi, R. Ghasemiasl, A.R. Majidian. Experimental analysis to improving thermosyphon (TPCT) thermal efficiency using nanoparticles/based fluids (water). European Phys. J. Plus., 132 (2017), 10.1140/epjp/i2017-11455-3

[8] T. Barbaryan, S. Hoseinzadeh, P. Heyns, M. Barbaryan. Developing a low-fluid pressure safety valve design through a numerical analysis approach. Int. J. Numer. Meth. Heat Fluid Flow, 30 (3) (2019), pp. 1427-1440, 10.1108/HFF-06-2019-0508
[9] S. Hoseinzadeh, P.S. Heyns, A.J. Chamkha, A. Shirkhani. Thermal analysis of porous fins enclosure with the comparison of analytical and numerical methods. J. Therm. Anal. Calorim., 138 (2019), pp. 727-735, 10.1007/s10973-019-08203-x
[10] S. Hoseinzadeh, R. Ghasemiasl, D. Havaei, A.J. Chamkha. Numerical investigation of rectangular thermal energy storage units with multiple phase change materials. J. Mol. Liq., 271 (2018), pp. 655-660
[11] J. Wannenburg, P.S. Heyns, A.D. Raath. Application of a fatigue equivalent static load methodology for the numerical durability assessment of heavy vehicle structures. Int. J. Fatigue, 31 (10) (2009), pp. 1541-1549
[12] L. Ge, W. Jiang, Y. Wang, S.T. Tu. Creep-fatigue strength design of plate-fin heat exchanger by a homogeneous method. Int. J. Mech. Sci., 146 (2018), pp. 221-233
[13] S.S. Pande, P.D. Darade, G. Gogate. Transient analysis and fatigue life prediction of tubesheet. Int. J. Res. Eng. Technol., 3 (09) (2014), pp. 464-471
[14] R.T.K. Raj, S. Ganne. Shell side numerical analysis of a shell and tube heat exchanger considering the effects of baffle inclination angle on fluid flow. Therm. Sci., 16 (4) (2012), pp. 1165-1174
[15] P. Arora, P.K. Singh, V. Bhasin, K.K. Vaze, A.K. Ghosh, D.M. Pukazhendhi, G. Raghava. Predictions for fatigue crack growth life of cracked pipes and pipe welds using RMS SIF approach and experimental validation. Int. J. Press. Vessels Pip., 88 (10) (2011), pp. 384-394
[16] C. Booysen, P.S. Heyns, M.P. Hindley, R. Scheepers. Fatigue life assessment of a low pressure steam turbine blade during transient resonant conditions using a probabilistic approach. Int. J. Fatigue, 73 (2015), pp. 17-26
[17] G.H. Farrahi, M. Chamani, A. Kiyoumarsioskouei, A.H. Mahmoudi. The effect of plugging of tubes on failure of shell and tube heat exchanger. Eng. Fail. Anal., 104 (2019), pp. 545-559
[18] G.H. Farrahi, K. Minaei, M. Chamani, A.H. Mahmoudi. Effect of Residual Stress on Failure of Tube-to-tubesheet Weld in Heat Exchangers. Int. J. Eng. (IJE) IJE Trans. A: Basics, 32 (1) (2019)
[19] A. Gupta, R. Kumar, A. Gupta. Condensation of R-134a inside a helically coiled tube-in-shell heat exchanger. Exp. Therm Fluid Sci., 54 (2014), pp. 279-289
[20] A.K. Solanki, R. Kumar. Condensation of R-134a inside micro-fin helical coiled tube-in-shell type heat exchanger. Exp. Therm Fluid Sci., 93 (2018), pp. 344-355
[21] E. Ozden, I. Tari. Shell side CFD analysis of a small shell-and-tube heat exchanger. Energy Convers. Manage., 51 (5) (2010), pp. 1004-1014
[22] A. Rondon, S. Guzey. Fatigue evaluation of the api specification 12f shop welded flat bottom tanks. Int. J. Press. Vessels Pip., 149 (2017), pp. 14-23
[23] H. Shiraiwa, Y. Kita. Performance improvement of a falling-film-type heat exchanger by insertion of shafts with screw blade in a heat exchanger tube. Appl. Therm. Eng., 102 (2016), pp. 55-62
[24] J. Wajs, M. Bajor, D. Mikielewicz. Thermal-hydraulic studies on the shell-and-tube heat exchanger with minijets. Energies, 12 (17) (2019), p. 3276
[25] R. Patil, S. Anand. Thermo-structural fatigue analysis of shell and tube type heat exchanger. Int. J. Pressure Vessels Piping, 155 (2017), pp. 35-42
[26] ASME. VIII, Division 2, Alternative Rules, Rules for Construction of Pressure Vessels, Design by analysis approach, 2015 Edition.

[27] S. Hoseinzadeh, S. Otaghsara, M. Khatir, P. Heyns. Numerical investigation of thermal pulsating alumina/water nanofluid flow over three different cross-sectional channel. International Journal of Numerical Methods for Heat & Fluid Flow (2019), 10.1108/HFF-09-2019-0671 ahead-of-print
[28] S. Hoseinzadeh, P. Heyns, H. Kariman. Numerical investigation of heat transfer of laminar and turbulent pulsating Al2O3/water nanofluid flow. Int. J. Numer. Meth. Heat Fluid Flow, 30 (3) (2019), pp. 1149-1166, 10.1108/HFF-06-2019-0485
[29] S. Hoseinzadeh, A. Bahrami, S.M. Mirhosseini, A. Sohani, P.S. Heyns. A Detailed experimental airfoil performance investigation using an equipped wind tunnel. Flow Meas. Instrum., 101717 (2020)